JOURNAL OF Applied Polymer SCIENCE

Polypyrrole-wrapped Pd nanoparticles hollow capsules as a catalyst for reduction of 4-nitroaniline

Hanzhi Zou, Mengyin Shang, Guohong Ren, Wenqin Wang
Faculty of Materials Science and Chemical Engineering, Ningbo University, Ningbo 315211, China
Correspondence to: W. Wang (E-mail: wqwang@126.com)

ABSTRACT: In this study, by *in situ* reduction of Pd^{2+} ions attached on the surface of the sulfonated polystyrene (PS-SO_3H) spheres, complete and dense palladium (Pd) nanoparticles (NPs) layer were deposited around PS-SO_3H spheres. The PS@Pd spheres were wrapped by polypyrrole (PPy) shell, which could avoid escaping of Pd NPs. After selectively etching the PS core, the hollow structures with Pd NPs embedded in PPy capsule shell were obtained. The as-prepared Pd@PPy hollow capsules showed excellent catalytic activity toward the reduction of 4-nitroaniline because of the high Pd NPs loading. Furthermore, good reusabilty was demonstrated seven times without any detectible loss in activity. © 2016 Wiley Periodicals, Inc. J. Appl. Polym. Sci. **2016**, *133*, 43933.

KEYWORDS: catalysts; colloids; composites; conducting polymers

Received 10 March 2016; accepted 15 May 2016
DOI: 10.1002/app.43933

INTRODUCTION

Noble metal (Au, Ag, Pd) nanoparticles (NPs) have drawn much attention due to their high catalytic activities toward different types of reactions.[1–3] However, their applications suffer from the aggregations caused by high surface energy and difficult separation due to their small size. Although anchoring metal NPs on supports to form core/shell-structured composites had been proven to be an effective method to solve above drawbacks,[4–8] the noble metal NPs decorated on the surface of supports might escape outside during catalytic procedures, which resulted to low reusability. To overcome this disadvantage, recently, some efforts have been made to fabricate multilayer-structured composites.[9–16] This strategy involved loading metal NPs on the supports (cores), followed deposition of another layer material on the surface of supports/metal composites. For example, Yin's group prepared a novel Fe_3O_4@SiO_2-Au@mesoporous SiO_2 catalyst.[9] The outermost SiO_2 shell not only avoided the leaching of the metal NPs but also allowed the diffusion of the chemical species to metal NPs in catalytic reactions. Besides mesoporous silica layer, conducting polymer-polypyrrle (PPy) is also proved to be an ideal shell material and the PPy shell wrapped the metal NPs did not weaken the catalytic activity of relevant catalysts.[17] For example, Yao et al. used polystyrene (PS) spheres as cores to adsorb Au NPs, followed deposition of PPy shell. The as-prepared composites exhibited good catalytic activity toward methylene blue dye.[18] In spite of recent popularity, in this multilayer-structured composite system, loading of metal NPs on the surface of the supports (cores) usually based on the electrostatic attraction between the metal NPs and supports. In most cases, low loading density of metal NPs on the supports surface was observed due to the weak interaction between metal NPs and supports and the strong electrostatic repulsion of the metal NPs. Therefore, obtaining high loading of metal in multilayer-structured composite is still a challenge.

Herein, we prepared a PPy-wrapped PS@Pd composite with high Pd loading. High loading of Pd NPs could be realized by the attraction of Pd^{2+} ion on the sulfonated polystyrene (PS-SO_3H) spheres, followed the *in situ* reduction using $NaBH_4$. PPy shell was wrapped around the PS-SO_3H@Pd spheres surface and the Pd@PPy hollow capsules could be obtained by etching the PS core with tetrahydrofuran (THF). The application of the as-prepared Pd@PPy hollow capsules as catalysts was investigated, and relevant results showed that the high Pd loading and hollow structures could effectively promote catalytic activity and reusabilty of the catalyst.

EXPERIMENTAL

Materials

Poly(vinyl pyrrolidone) (PVP, $M_w = 550{,}000$) was purchased from Sigma-Aldrich. Azoisobutyronitrile (AIBN), styrene, $PdCl_2$(≥99.8%), NH_4OH (25%), concentrated sulfuric acid, sodium borohydride, pyrrole, $FeCl_3$•$6H_2O$, anhydrous ethanol and 4-nitroaniline were obtained from Sinopharm Chemical

Additional Supporting Information may be found in the online version of this article.

Reagent Co. (Shanghai, China). AIBN was crystallized again. Styrene and pyrrole were distilled under reduced pressure before being used. Other chemicals were used as received.

Fabrication of PS-SO_3H@Pd Spheres

Synthesis of PS spheres and relevant sulfonation process were carried out according to the previous reports (see Supporting Information).[19,20] 17.5 mg of the as-obtained PS-SO_3H spheres and 7.2 mg of $PdCl_2$ were added into 20 mL of deionized water and the above mixed solution was heated to 60 °C under stirring. After 1 h, the solution was centrifuged and the precipitate was redispersed in 20 mL of deionized water. Then, 2 mL of $NaBH_4$ (30 mg) aqueous solution was added, and the reaction was allowed to proceed for 1 h. Finally, the resultant product was separated by centrifugation and washed with deionized water three times.

Fabrication of PS-SO_3H@Pd@PPy Spheres and Pd@PPy Hollow Capsules

The as-prepared PS-SO_3H@Pd spheres were dispersed in 20 mL of deionized water and 35 mg of PVP was added under stirring. After 24 h, the mixed solution was centrifuged and the precipitate was washed with deionized water to remove the nonadsorptive PVP. The PS-SO_3H@Pd spheres adsorbing PVP were redispersed in 30 mL of deionized water; then, 15 μL of pyrrole was added. The mixture was kept stirring at 200 rpm in an ice bath for 3 h. Subsequently, $FeCl_3 \cdot 6H_2O$ (0.5 g in 5 mL of deionized water) was dropped to above suspension. This reaction was allowed to proceed for 6 h under stirring and the entire system was kept in an ice bath. Finally, the resultant dark-green powder was separated by centrifugation and washed three times with ethanol. To remove PS cores, the as-made PS-SO_3H@Pd@PPy spheres were suspended into 20 mL of THF solution. After stirring 48 h, the resulting Pd@PPy hollow capsules were separated and washed with ethanol.

Catalytic Performance

The catalytic reduction of 4-nitroaniline (4-NA) was performed in a 3 mL quartz cuvette at room temperature. Three hundred microliter of 1.0 $\times 10^{-3}$ *M* 4-NA stock solution and 300 μL of 0.1 *M* ice-cold $NaBH_4$ solution were added into 2.4 mL of water and stirred for 1 min. Then, the catalysts, PS-SO_3H@Pd@PPy spheres and Pd@PPy hollow capsules were added into above mixed solution. The progress of the reaction was monitored with the UV-vis spectrophotometer (UV-2600, Shimadzu) and the absorption spectra were recorded.

Characterization

The morphologies of samples were observed by transmission electron microscope (TEM, H-7650) and field-emission scanning electron microscopy (FE-SEM, SU70). Fourier-transform infrared spectroscopy (FT-IR 6700, Nicolet) was used to characterize chemical information of the products. The composition of the samples was analyzed using X-ray photoelectron spectroscopy (XPS, Axis Ultra dld). The phase and the crystallographic structure of the products were characterized by X-ray diffraction (XRD) on a Rigaku D/max-RA XRD meter. Thermogravimetric analysis (TGA) was determined with a Perkin-Elmer thermogravimetric analyzer (TG-DTA, SSC-5200) at a heating rate of 10 °C/min in N_2 form room temperature up to 750 °C.

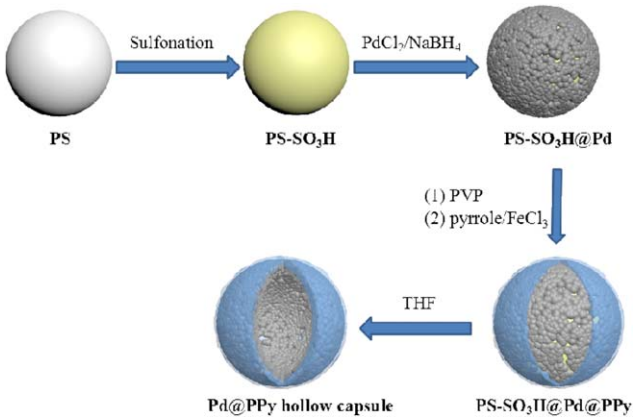

Scheme 1. Schematic illustration of the synthetic procedure for generating PS-SO3H@Pd@PPy and Pd@PPy hollow capsules. [Color figure can be viewed in the online issue, which is available at wileyonlinelibrary.com.]

RESULTS AND DISCUSSION

The fabrication procedure of the Pd@PPy hollow capsules is illustrated in Scheme 1. PS spheres were sulfonated, and Pd^{2+} ions were attached on the PS spheres with sulfuric groups. After the addition of $NaBH_4$, dense Pd NPs were deposited around PS-SO_3H spheres. PVP adsorbed on the PS-SO_3H@Pd spheres provided active sites for pyrrole monomer loading. In the presence of $FeCl_3$, pyrrole monomer was polymerized, and PPy layer was wrapped around the PS-SO_3H@Pd spheres surface. Finally, the PS core was selectively dissolved with THF. As THF is a good solvent for PS but a poor solvent for PPy,[21] we could obtain Pd@PPy hollow capsules by selectively removal of the PS cores with THF.

Figure 1 shows the SEM images of PS spheres, PS-SO_3H@Pd spheres, PS-SO_3H@Pd@PPy spheres, and Pd@PPy hollow capsule. In Figure 1(A,a), the as-made PS spheres exhibit smooth surface and narrow size distribution with a size of about 2.7 μm in diameter. When Pd^{2+} ions attached on PS-SO_3H spheres were reduced by $NaBH_4$, except few unavoidable aggregations of Pd NPs, a homogeneous and dense Pd NPs layer was observed from Figure 1(B,d) and Figure S1 (see Supporting Information). In Figure 1(C,c), the PS-SO_3H@Pd@PPy spheres show a considerably rough surface, which is the feature of the PPy homopolymer.[18,22] From Figure 1(D,d), it is found that when the PS core was removed, the relevant products still remained their spherical contour, which indicated the PPy shell had enough mechanical strength to maintain the hollow structure. In this study, we also found that the control of the dosages of $PdCl_2$ and pyrrole was essential for obtaining the well-defined Pd NPs layer and PPy shell. More amount of $PdCl_2$ and pyrrole resulted into significant aggregation of Pd NPs and polymerization of the partial pyrrole monomer in solution, respectively (see Supporting Information, Figure S2 and Figure S3).

TEM was used to further examine the microstructures of the samples. Compared to Figure 2(a), Figure 2(b) shows slightly rough surface owing to the presence of tiny Pd NPs on the PS-SO_3H spheres surface. Much rougher surface is observed in Figure 2(c), when pyrrole monomer was polymerized around PS-

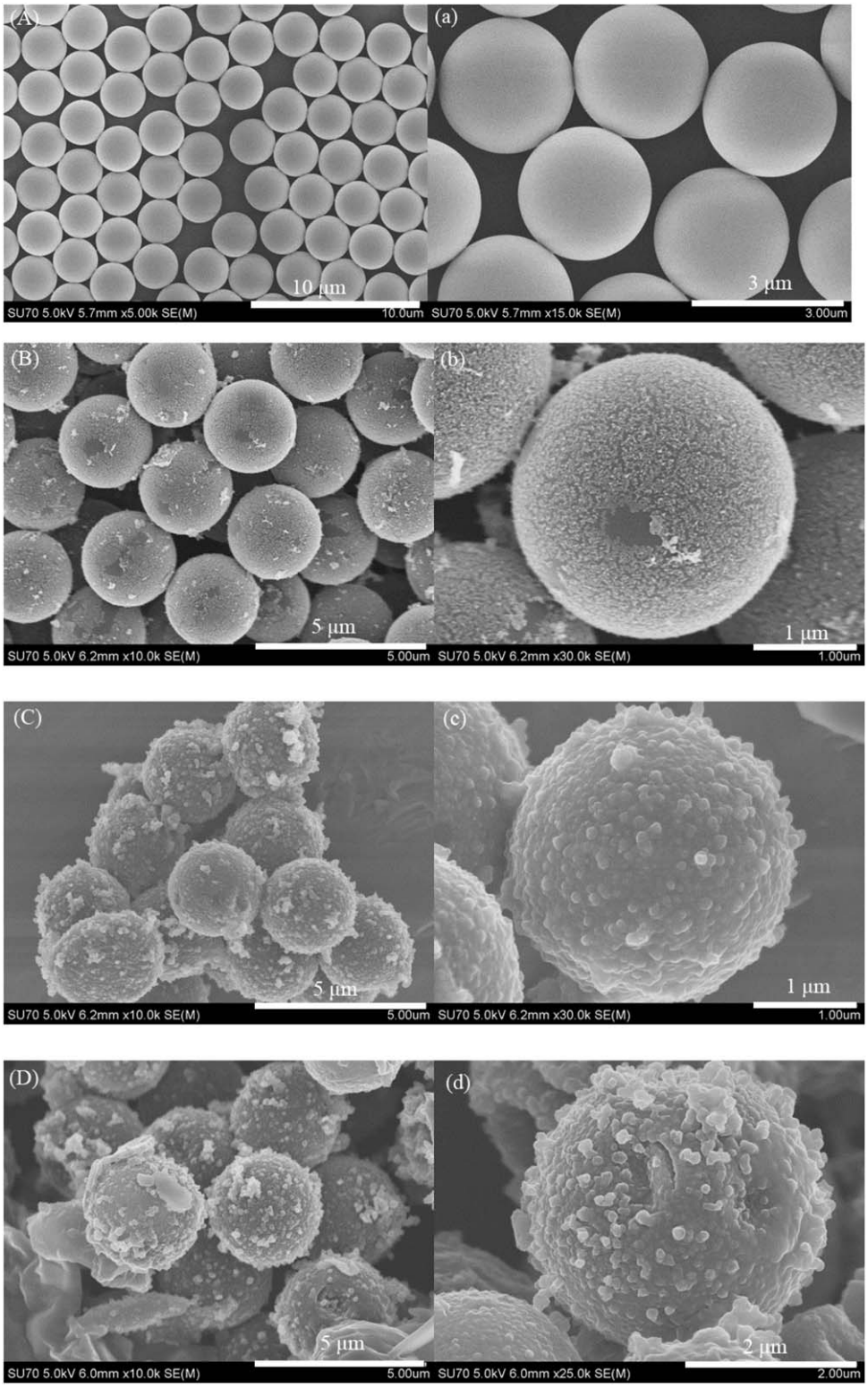

Figure 1. Low-and high magnification SEM images of the samples: (A,a) PS spheres, (B,b) PS-SO_3H@Pd spheres, (C,c) PS-SO_3H@Pd@PPy spheres, (D,d) Pd@PPy hollow capsules.

SO_3H@Pd spheres. These results are in good agreement with the observations from the SEM images. After removal of PS core, Figure 2(d) confirms that the relevant products possess a well-defined hollow structure with an outer shell.

The XRD patterns of the samples were shown in Figure 3. Figure 3(a) shows a very broad peak at 19.8°, which is attributed to the PS.[23] Figure 3(b) displays four diffraction peaks at $2\theta = 39.8$, 46.1, 67.7, and 81.6°, which are corresponded to

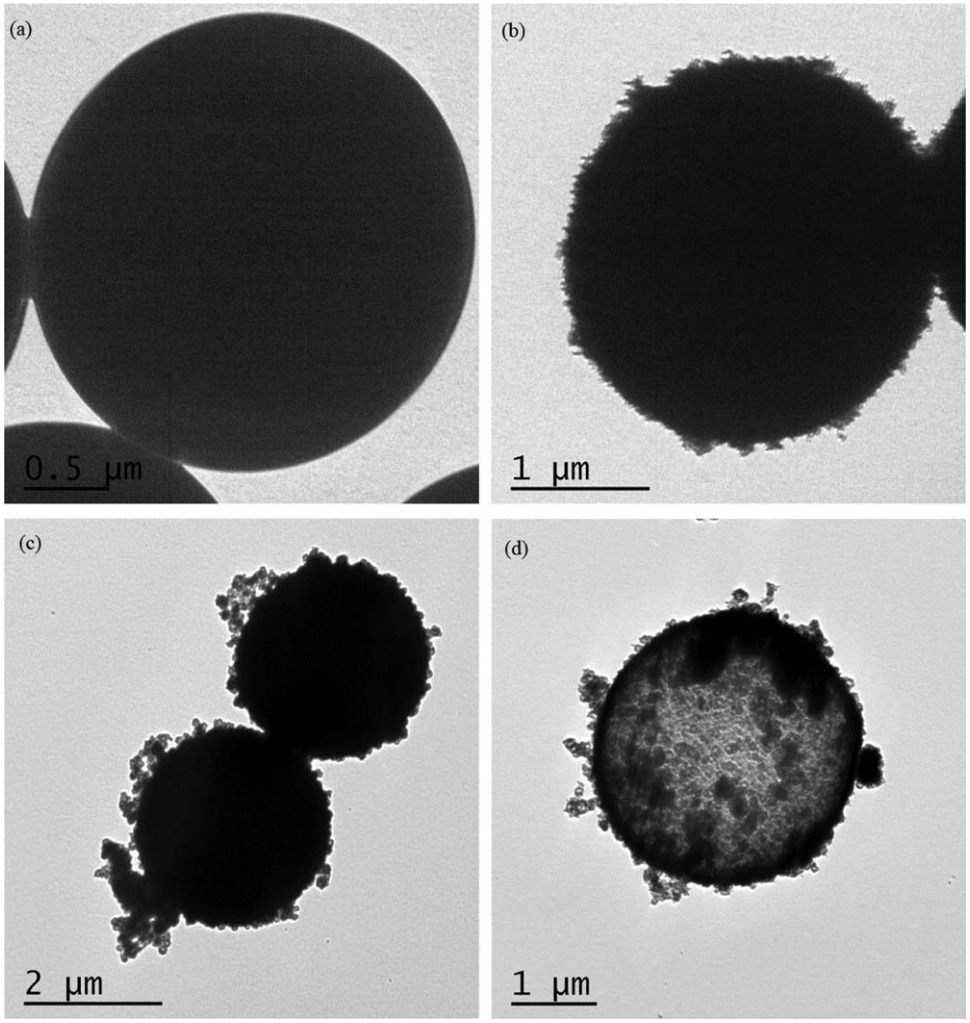

Figure 2. TEM images of the samples: (a) PS spheres, (b) PS-SO_3H@Pd spheres, (c) PS-SO_3H@Pd@PPy spheres, (d) Pd@PPy hollow capsules.

(111), (200), (220), and (311) Bragg reflections of Pd crystals, respectively. The positions of all the sharp peaks are in good agreement with those reported for Pd NPs,[12] indicating Pd NPs have been loaded on the PS spheres surface. The XRD pattern of PS-SO_3H@Pd@PPy is shown in Figure 3(c), the same diffraction peaks of Pd compared with Figure 3(b) are observed, confirming the Pd NPs have been successfully wrapped by PPy layer. Figure 3(d) shows the XRD pattern of Pd@PPy hollow capsules and the broad peak of PS is not observed, which indicates PS core have been completely removed.

The molecular structures of the PS-SO_3H spheres and Pd@PPy hollow capsules were characterized by FT-IR. Figure 4 shows the FT-IR spectra of the products. In Figure 4(a), the characteristic peaks of PS component are found at about 1495, 1454, 755, and 698 cm^{-1}, and one broad absorption band centered at 1179 cm^{-1} is assigned to the ν(S═O) stretching modes of aromatic sulfonic acid.[24,25] In Figure 4(b), the peak located at about 1653 cm^{-1} is assigned to the coupling between C-C and the unsymmetrical stretching vibration of the pyrrole rings.[26] The peaks at 1548 and 1450 cm^{-1} are attributed to the pyrrole ring-stretching and the conjugated C—N stretching mode, respectively. 1162 cm^{-1} is assigned to the C—N stretching mode, and 785 cm^{-1} is attributable to C—H wagging vibration.[27,28] Above results demonstrate that the capsules shell contains PPy. In addition, the characteristic peaks of PS component

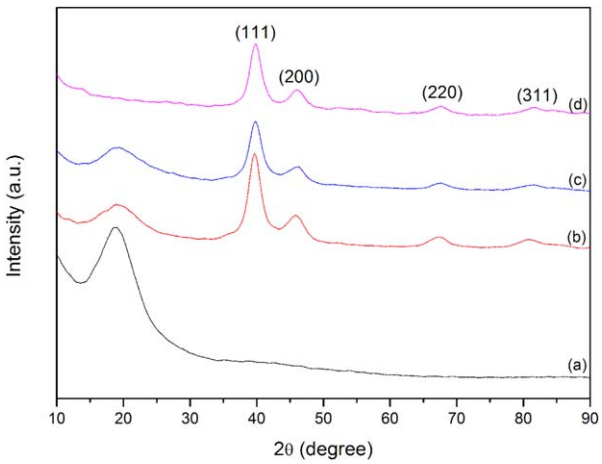

Figure 3. XRD patterns of: (a) PS-SO_3H spheres, (b) PS-SO_3H@Pd spheres, (c) PS-SO_3H@Pd@PPy spheres, and (d) Pd@PPy hollow capsules. [Color figure can be viewed in the online issue, which is available at wileyonlinelibrary.com.]

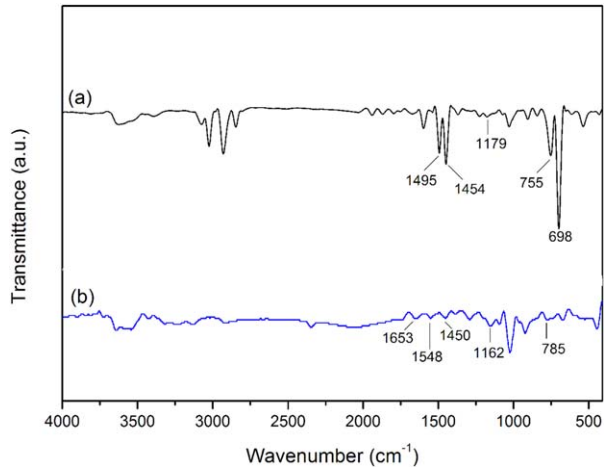

Figure 4. The FT-IR spectra of: (a) PS-SO_3H spheres, (b) Pd@PPy hollow capsules. [Color figure can be viewed in the online issue, which is available at wileyonlinelibrary.com.]

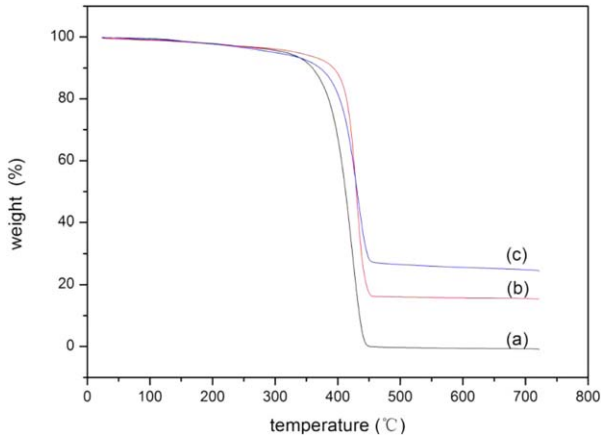

Figure 6. TGA of samples: (a) PS-SO_3H spheres, (b) PS-SO_3H@Pd spheres, and (c) PS-SO_3H@Pd@PPy spheres. [Color figure can be viewed in the online issue, which is available at wileyonlinelibrary.com.]

are not observed in Figure 4(b), indicating the PS cores have been completely removed with THF.

XPS was also used to further characterize the chemical structures of the products. The XPS survey scans of the PS-SO_3H@Pd@PPy spheres is shown in Figure 5(a). Peaks corresponding to oxygen, nitrogen, palladium, and carbon are clearly observed. In Figure 5(b), the Pd binding energy of PS-SO_3H@Pd@PPy spheres shows two strong peaks centered at 335.5eV and 340.5 eV, respectively, which are in good agreement with the reported XPS data of Pd $3d_{5/2}$ and Pd $3d_{3/2}$ in metallic Pd.[29]

The TGA results are shown in Figure 6. Curves a, b, and c correspond to the sample PS-SO_3H spheres, PS-SO_3H@Pd spheres, and PS-SO_3H@Pd@PPy spheres, respectively. The weight loss below 200 °C is attributed to the evaporation of water and residual organic solvent. In curve a, PS begins decomposing at about 380 °C, and PS completely vanishes when the temperature reaches about 450 °C. Comparing curve b with curve a, the decomposed temperature of PS is up to 410 °C due to the presence of Pd NPs shell. In curve b, the content of residuals (Pd NPs) is about 16.2 wt%. From curve c, it is found that the residue percentages of PS-SO_3H@Pd@PPy spheres after TG analysis in air are 25.7% because PPy cannot be completely decomposed in air and is carbonized to form graphitic structures.[30]

The catalytic performance of the PS-SO_3H@Pd@PPy spheres and Pd@PPy hollow capsules were examined by catalyzed reduction of 4-nitroaniline(4-NA) to p-phenylene diamine (p-PDA) in the presence of $NaBH_4$. The reaction rate was monitored by successive UV-vis absorbance measurements of the reaction solution as 4-NA and p-PDA exhibited distinct peaks at 380 and 238 nm, respectively. Compared Figure 7(a) with Figure 7(b), it is found that in the presence of the Pd@PPy hollow capsules, the reaction is faster than that using PS-SO_3H@Pd@PPy spheres as catalysts because the hollow structure promotes diffusion and mass transfer of reactants.[12] As the initial concentration of reducing agent $NaBH_4$ is much higher as compared to 4-NA, the catalytic reaction follows the pseudo-first-order reaction kinetics.[31,32] Therefore, the apparent rate constant (k/s) in the catalytic reductions is calculated using the following equation:

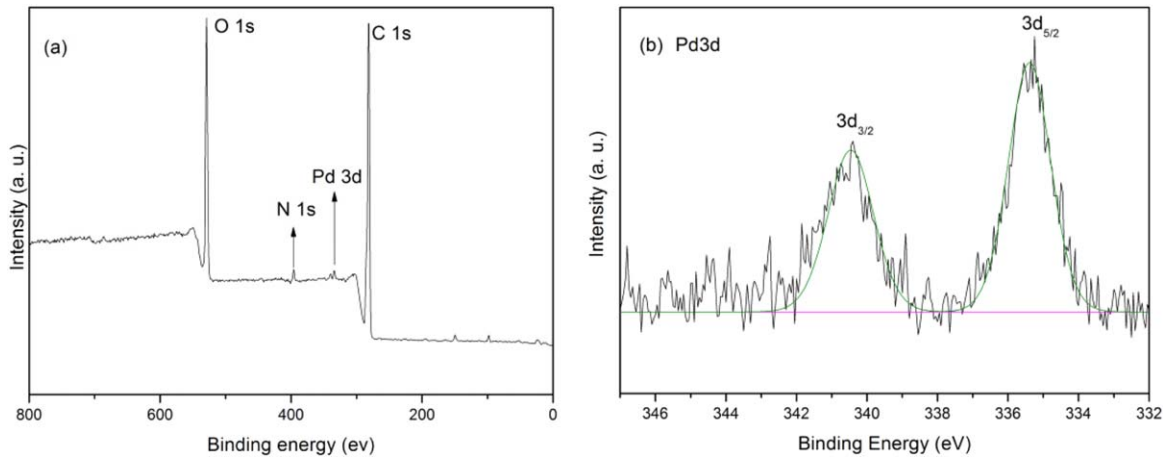

Figure 5. XPS spectra of: (a) PS-SO_3H@Pd@PPy spheres, (b) Pd 3d of PS-SO_3H@Pd@PPy spheres. [Color figure can be viewed in the online issue, which is available at wileyonlinelibrary.com.]

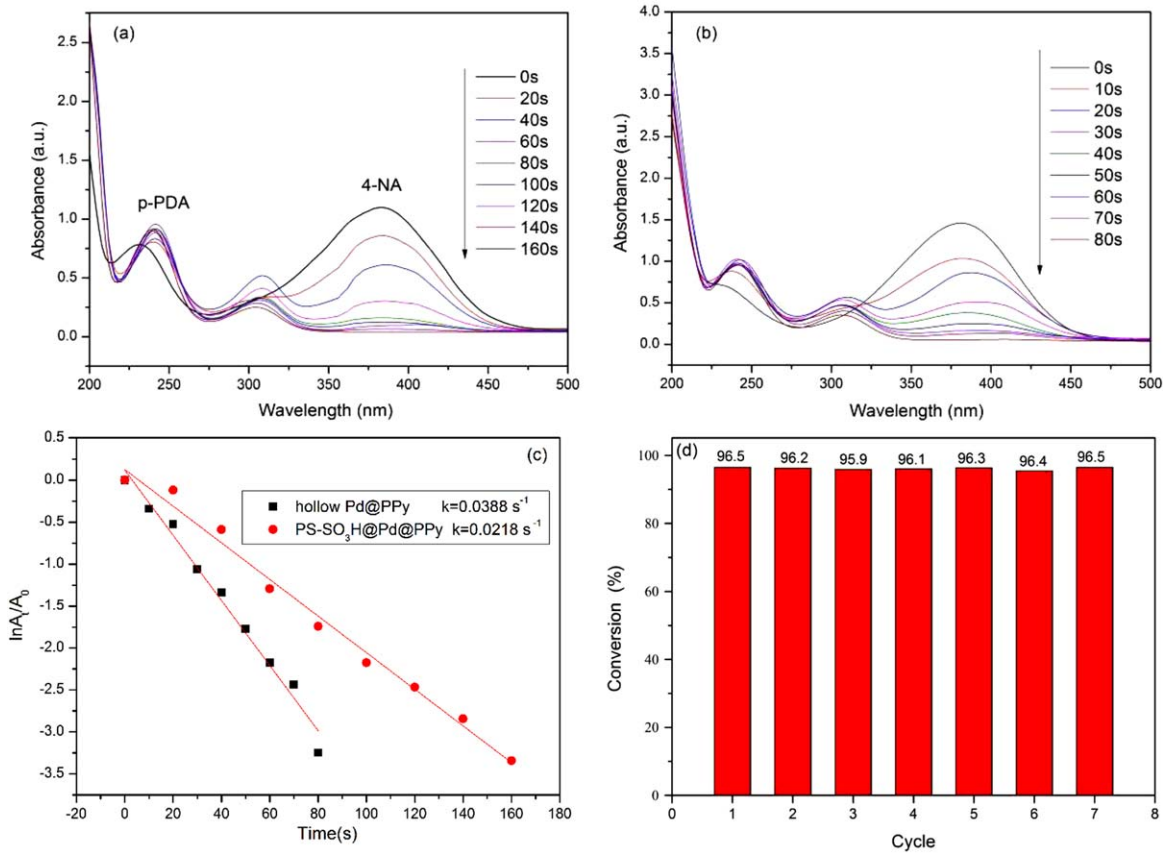

Figure 7. (a) Time-dependent UV-vis spectra of the reduction of 4-NA to p-PDA catalyze by PS-SO_3H@Pd@PPy spheres, (b) Time-dependent UV-vis spectra of the reduction of 4-NA to p-PDA catalyze by Pd@PPy hollow capsules, (c) Plot of logarithm of (A_t/A_0) at 380 nm versus reduction time with different catalysts, (d) conversion of 4-NA in seven successive cycles of reduction with Pd@PPy hollow capsules. [Color figure can be viewed in the online issue, which is available at wileyonlinelibrary.com.]

$$\ln(A_t/A_0) = -kt$$

where A_t is the absorbance of 4-NA at time t, and A_0 is the absorbance of 4-NA at time 0. The pseudo-first-order rate constant (k) was calculated from the slop of plot of $\ln(A_t/A_0)$ versus time [Figure 7(c)]. The rate constant (k) was calculated to be 2.18 $\times$ 10^{-2} s^{-1} and 3.88 $\times 10^{-2}$ s^{-1}, respectively. The k value of Pd@PPy hollow capsules catalyst is higher than that of PS-SO_3H@Pd@PPy catalyst. In addition, because of high Pd loading in catalyst, above both values are also far higher than that reported by other research group.[13] The reusability of the Pd@PPy hollow capsules catalyst was also examined and seven successive catalytic reactions were carried out. The results in Figure 7(d) show that no significant decrease in catalytic activity of Pd@PPy hollow capsules is detected, which indicates the catalyst has good reusability. This result also indirectly confirms Pd NPs are embedded in the capsules shell, which makes Pd NPs hardly escape from the capsules and is favorable for remain catalytic properties of Pd NPs in catalytic reaction.

CONCLUSIONS

In conclusion, we reported the synthesis of Pd@PPy hollow capsules with high Pd loading and good catalytic activity. Dense Pd NPs shell could be obtained by the attraction between Pd^{2+} and PS-SO_3H spheres, followed the *in situ* reduction by $NaBH_4$. PPy layer was deposited around the PS-SO_3H@Pd spheres surface and Pd NPs were embedded in the PPy shell, which avoided escaping of Pd NPs in catalytic reaction. After removal of PS cores, the obtained Pd@PPy hollow capsules exhibited excellent catalytic activity and good reusability.

ACKNOWLEDGMENTS

This work was sponsored by K.C. Wong Magna Fund in Ningbo University, Fund for Science and Technology Innovative Team in Zhejiang Province (2011R50001-03), Ningbo Natural Science Foundation (2014A610142), and Ningbo Key Laboratory of Specialty Polymers (2014A22001).

REFERENCES

1. Daniel, M. C.; Astruc, D. *Chem. Rev.* **2004**, *104*, 293.
2. Hervés, P.; Pérez-Lorenzo, M.; Liz-Marzán, L. M.; Dzubiella, J.; Lu, Y.; Ballauff, M. *Chem. Soc. Rev.* **2012**, *41*, 5577.
3. Chen, A.; Ostrom, C. *Chem. Rev.* **2015**, *115*, 11999.
4. Zhang, H.; Zhong, X.; Xu, J. J.; Chen, H. Y. *Langmuir* **2008**, *24*, 13748.
5. Deng, Z. W.; Chen, M.; Wu, L. M. *J. Phys. Chem. C* **2007**, *111*, 11692.

6. Chaudhuri, R. G.; Paria, S. *Chem. Rev.* **2012**, *112*, 2373.
7. Deng, Z. W.; Zhu, H. B.; Peng, B.; Chen, H.; Sun, Y. F.; Gang, X. D.; Jin, P. J.; Wang, J. L. *ASC Appl. Mater. Interfaces* **2012**, *4*, 5625.
8. Khakyzadeh, V.; Luque, R.; Zolfigol, M. A.; Vahidian, H. R.; Salehzadeh, H.; Moradi, V.; Soleymani, A. R.; Moosavi-Zare, A. R.; Xu, K. *RSC Adv.* **2015**, *5*, 3917.
9. Ge, J. P.; Zhang, Q.; Zhang, T. R.; Yin, Y. D. *Angew. Chem. Int. Ed.* **2008**, *47*, 8924.
10. Wang, Y. F.; Biradar, A. V.; Duncan, C. T.; Asefa, T. *J. Mater. Chem.* **2010**, *20*, 7834.
11. Han, J.; Lu, S.; Jin, C. J.; Wang, M. G.; Guo, R. *J. Mater. Chem. A* **2014**, *2*, 13016.
12. Zhang, N.; Xu, Y. J. *Chem. Mater.* **2013**, *25*, 1979.
13. Kong, L. R.; Lu, X. F.; Jin, E.; Jiang, S.; Bian, X. J.; Zhang, W. J.; Wang, C. *J. Solid State Chem.* **2009**, *182*, 2081.
14. Zhang, Q.; Ge, J. P.; Goebl, J.; Hu, Y. X.; Sun, Y. G.; Yin, Y. D. *Adv. Mater.* **2010**, *22*, 1905.
15. Huang, L.; Ao, L. J.; Xie, X. B.; Gao, G. H.; Foda, M. F.; Su, W. *Nanoscale* **2015**, *7*, 806.
16. Yao, T. J.; Zuo, Q.; Wang, H.; Wu, J.; Xin, B.; Cui, F.; Cui, T. Y. *J. Colloid Interface Sci.* **2015**, *450*, 366.
17. Zhang, X.; Lin, M.; Lin, X. Y.; Zhang, C. T.; Wei, H. T.; Zhang, H.; Yang, B. *ACS Appl. Mater. Interfaces* **2014**, *6*, 450.
18. Yao, T. J.; Cui, T. Y.; Wang, H.; Xu, L. X.; Cui, F.; Wu, J. *Nanoscale* **2014**, *6*, 7666.
19. Xiao, M. D.; Chen, H. J.; Ming, T.; Shao, L.; Wang, J. F. *ACS Nano* **2010**, *4*, 6565.
20. Cai, W. J.; Wang, W. Q.; Yang, Y. Q.; Ren, G. H.; Chen, T. *RSC Adv.* **2014**, *4*, 2295.
21. Bai, M. Y.; Cheng, Y. J.; Wickline, S. A.; Xia, Y. *Small* **2009**, *5*, 1747.
22. Xiao, H. M.; Zhang, W. D.; Wan, M. X.; Fu, S. Y. *J. Polym. Sci. Part A: Polym. Chem.* **2009**, *47*, 4446.
23. Fujii, S.; Matsuzawa, S.; Hamasaki, H.; Nakamura, Y.; Bouleghlimat, A.; Buurma, N. J. *Langmuir* **2012**, *28*, 2436.
24. Steenackers, M.; Lud, S. Q.; Niedermeier, M.; Bruno, P.; Gruen, D. M.; Feulner, P.; Stutzmann, M.; Garrido, J. A.; Jordan, R. *J. Am. Chem. Soc.* **2007**, *129*, 15655.
25. Yang, Y.; Chu, Y.; Yang, F. Y.; Zhang, Y. P. *Mater. Chem. Phys.* **2005**, *92*, 164.
26. Bai, Z. Y.; Yang, L.; Li, L.; Lv, J.; Wang, K.; Zhang, J. *J. Phys. Chem. C* **2009**, *113*, 10568.
27. Feng, X. M.; Sun, Z. Z.; Hou, W. H.; Zhu, J. J. *Nanotechnology* **2007**, *18*, 1956031.
28. Mathys, G. I.; Truong, V. T. *Synth. Met.* **1997**, *89*, 103.
29. Jin, Z.; Nackashi, D.; Lu, W.; Kittrell, C.; James, M. T. *Chem. Mater.* **2010**, *22*, 5695.
30. Jang, J.; Yoon, H. *Adv. Mater.* **2003**, *15*, 2088.
31. Mei, Y.; Lu, Y.; Polzer, F.; Ballauff, M. *Chem. Mater.* **2007**, *19*, 1062.
32. Wang, Y.; Wei, G. W.; Zhang, W. Q.; Jiang, X. W.; Zheng, P. W.; Shi, L. Q.; Dong, A. J. *J. Mol. Catal. A: Chem.* **2007**, *266*, 233.